Tellus (2005), 57B, 189–202
Printed in Singapore. All rights reserved

TELLUS

Vegetation–soil water interaction within a dynamical ecosystem model of grassland in semi-arid areas

By XIAODONG ZENG[1,2]*, XUBIN ZENG[1], SAMUEL S. P. SHEN[2], ROBERT E. DICKINSON[3] and QING-CUN ZENG[4], [1]*Department of Atmospheric Sciences, The University of Arizona, Tucson, AZ 85721, USA;* [2]*Department of Mathematical and Statistical Sciences, University of Alberta, Edmonton, AB T6G 2G1, Canada;* [3]*School of Earth and Atmospheric Sciences, Georgia Institute of Technology, Atlanta, GA 30332, USA;* [4]*Institute of Atmospheric Physics, Chinese Academy of Sciences, Beijing 100029, P. R. China*

(Manuscript received 20 July 2004; in final form 17 February 2005)

ABSTRACT

A dynamical ecosystem model with three variables, living biomass, wilted biomass and available soil wetness, is developed to examine the vegetation–soil water interaction in semi-arid areas. The governing equations are based on the mass conservation law. The physical and biophysical processes are formulated with the parameters estimated from observational data. Both numerical results and qualitative analysis of the model as well as observational data indicate that the maintenance of a grassland requires a minimum precipitation (or equivalently, a minimum moisture index), and the grassland and desert ecosystem can coexist when precipitation is within a range above this threshold. Sensitivity studies show that these numerical results are robust with respect to model parameters and the transformation functions. It is also found that the wilted vegetation plays a very important role in shaping the transition between grassland and desert. By using the theories of an attractor basin and multiple equilibrium states, the conditions for grassland maintenance and the strategy of grazing are also analysed.

1. Introduction

Land ecosystems are primarily determined by climatic conditions (sunlight, temperature, precipitation, CO_2 concentration, etc.) and soil properties (soil type, nutrient distribution). On the other hand, vegetation interacts with the environment (soil and surrounding atmosphere) through the exchange of energy, momentum and materials such as water vapour and various gases, and thus influences climatic variables such as temperature and precipitation. The study of these mutual interactions is an important issue for both regional and global climate changes.

Patterns of biosphere–geosphere interaction usually vary gradually within a homogeneous distributed ecosystem, but can undergo dramatic change over regions where multiple ecosystems (e.g. desert, grassland and forest) coexist. The triggering of the transition between different ecosystems as well as the features of the corresponding biosphere–geosphere interactions have been studied at various spatial and temporal scales. For example, analytically tractable simple models use the concept of equilibrium to represent a stable ecosystem, and show that the transition between different equilibrium states (corresponding to vegetation ecosystem and desert) can occur with changing climatic conditions such as carbon cycle (Svirezhev and von Bloh, 1997), temperature (Svirezhev and von Bloh, 1998) and precipitation (Brovkin et al., 1998). Conceptual and intermediate-level models have demonstrated grassland–desert transitions in the Sahel/Sahara region (Claussen et al., 1999; Zeng and Neelin, 2000; Wang and Eltahir, 2000a,b) and a possible forest–savanna transition over Amazonia (Oyama and Nobre, 2003). Dynamical global vegetation models (DGVM) also predicted the collapse of the Amazon forest in response to changing climate driven by an assumed doubling of CO_2 concentration in the next 50 yr (Cox et al., 2000; Huntingford et al., 2000). These models demonstrated that under certain conditions, subtle variations of climate could be strongly amplified by atmosphere–vegetation feedback and trigger an abrupt switch of ecosystem from one state to another.

Semi-arid climate regions are important systems for studying the biosphere–geosphere interaction, ecosystem transition and climate change. Transitions between desert and humid climates occur for a ratio of precipitation to potential evapotranspiration from 0.2 to 0.5 (UNEP, 1992). Over this range, the sunlight and temperature are usually sufficient to support grasses, but the precipitation is sparse and irregular so the soil water budget becomes the most important factor in influencing the growth of

*Corresponding author.
e-mail: xdzeng@atmo.arizona.edu

vegetation. For this reason, the existence of vegetation in this region is fragile. The studies of the Sahel/Sahara region referred to above have shown grassland–desert transitions due to the atmosphere–vegetation feedbacks. On the other hand, our earlier studies of the Inner Mongolia grassland/Gobi Desert show that the land system itself, under certain prescribed climatic conditions, could also possess multiple equilibrium states. We used a simple prognostic model with two state variables, i.e. the total biomass and soil wetness, to demonstrate the coexistence of grassland and desert under the prescribed constant precipitation (Zeng et al., 1994; Zeng and Zeng, 1996a) or for seasonal variable precipitation (Zeng and Zeng, 1996b). In a more recent study, we introduced a third state variable, i.e. the wilted biomass, to investigate its impact on the vegetation–soil interaction (Zeng et al., 2004). The main conclusion is that the shading of soil by living and wilted vegetation can effectively reduce the evaporation from the soil surface, and hence can conserve enough soil water for maintenance of vegetation in semi-arid areas.

This paper extends the brief study of Zeng et al. (2004) through a more comprehensive description of the model and its behaviour. The formulation of model processes and the estimation of the model parameters are discussed in Section 2. The multiple equilibrium states are demonstrated, and their stabilities are proved in Section 3. The robustness of the modelling results in terms of their sensitivity to both the model parameters and the transformation functions is discussed in Section 4. The mechanism of self-organization of vegetation and the vegetation–soil interaction is provided in Section 5 to explain the coexistence of grassland and desert in semi-arid areas. In particular, the influence of the wilted biomass in the vegetation–soil interaction is emphasized. In Section 6 the issues of grassland maintenance and the strategy of grazing are discussed. Finally, in Section 7, we discuss some empirical and practical issues, and compare our model with some other relevant models.

2. The dynamical grassland model

2.1. The three state variables and their conservation equations

Our model of grassland considers a single vertical column of soil and one species of grass, and it includes three state variables, the mass density of living leaves x (kg m^{-2}), the available soil wetness y (in the rooting zone) (kg m^{-2}, or mm) and the mass density of wilted (littered) leaves z (kg m^{-2}). The conservation of these variables can be written as:

$$\mathrm{d}x/\mathrm{d}t = F_1 = G(x, y) - D(x, y) - C(x) \tag{1}$$

$$\mathrm{d}y/\mathrm{d}t = F_2 = P - E_\mathrm{v}(x, y, z) - E_\mathrm{t}(x, y) - R(x, y, z) \tag{2}$$

and

$$\mathrm{d}z/\mathrm{d}t = F_3 = G_z(x, y) - D_z(z) - C_z(z), \tag{3}$$

where G, D and C are the growth (net primary productivity, i.e. photosynthesis minus plant growth respiration), wilting and consumption (grazing) of the living leaves, G_z, D_z and C_z are the accumulation, decomposition and consumption of the wilted leaves, P is the prescribed precipitation (more accurately, P is through fall, i.e. precipitation minus water intercepted by live and wilted leaves), E_v is soil evaporation, E_t is vegetation transpiration and R is runoff.

2.2. Formulation of the processes in eqs (1)–(3)

All terms on the right-hand side of eqs (1)–(3), except for the consumptions, depend on sunlight, atmospheric conditions, soil properties and physiological–biophysical characteristics of grass. In general, the functional form $f(u)$ of any state variable u needs to satisfy two constraints

$$f(u \to \infty) \to f_\mathrm{max} \text{ (the saturated limit)} \tag{4}$$

and

$$f(u \to 0) \sim f_\mathrm{max} k u \text{ (the linear limit)}, \tag{5}$$

where f_max and k are constants, while the transition behaviour between these two limits can be very complicated. The exponential function

$$f_1(u) = f_\mathrm{max}(1 - \mathrm{e}^{-ku}) \tag{6}$$

is often used in ecological and meteorological studies (e.g. Serafini and Sud, 1987; Haxeltine and Prentice, 1996; Zeng and Neelin, 2000) as a model to connect the two limits of eqs (4) and (5). It is also used in our model. Besides this class of exponential transformation function denoted by f_1, other transformation functions will also be considered (see Section 4.2).

The growth term G depends on the balance of photosynthesis and growth respiration. The photosynthate by the living leaves can be written as (Dickinson et al., 1998)

$$G_\mathrm{p} = \alpha_0 P_\mathrm{c} L_\mathrm{ef}, \tag{7}$$

where P_c is the rate of carbon assimilation per unit leaf area and L_ef is the sunlit leaf area index and can be expressed as (Campbell and Norman, 1998, eq. (15.23); see also, Haxeltine and Prentice, 1996; Huntingford et al., 2000)

$$L_\mathrm{ef} = (1 - \mathrm{e}^{-K\mathrm{LAI}})/K, \tag{8}$$

where K is a constant and LAI is the leaf area index which is proportional to the living biomass (x). The coefficient α_0 depends on the soil water content and can be written as

$$\alpha_0 \propto (1 - \mathrm{e}^{-K'y}). \tag{9}$$

Also the growth respiration of living biomass is assumed to be proportional to the photosynthate, $G_\mathrm{r} \propto G_\mathrm{p}$ (Dickinson et al., 1998). Therefore the growth term G can be formulated as

$$G = G_\mathrm{p} - G_\mathrm{r} = \alpha(1 - \mathrm{e}^{-\varepsilon_\mathrm{gx} x})(1 - e^{-\varepsilon_\mathrm{gy} y}), \tag{10}$$

where α is the maximum growth rate depending on the climatic condition, soil and grass species properties, and ε_{gx} and ε_{gy} are exponential attenuation coefficients.

The death, i.e. wilting, term D can be derived similarly. In contrast to G, however, it is expected that $D(x \to \infty) \to \infty$ due to the space competition and $D(y \to 0) \to \infty$ due to the stress of drought. Thus, D can be formulated as

$$D = \beta(\mathrm{e}^{\varepsilon_{dx}x} - 1)(1 - \mathrm{e}^{-\varepsilon_{dy}y})^{-1}, \tag{11}$$

where β is the characteristic wilting rate. Similarly, D_z is written as

$$D_z = \beta_z\,(\mathrm{e}^{\varepsilon_{dz}z} - 1)\,, \tag{12}$$

where β_z is the characteristic rate of wilted biomass decomposition. The accumulation of wilted biomass, G_z, should be proportional to D, i.e.

$$G_z = \alpha_z D = \alpha_z \beta(\mathrm{e}^{\varepsilon_{dx}x} - 1)(1 - \mathrm{e}^{-\varepsilon_{dy}y})^{-1}, \tag{13}$$

where $\alpha_z (0 \le \alpha_z < 1)$ is the rate of accumulation of wilted biomass.

For simplicity, the consumption terms C and C_z are assumed to be zero. The issue of grazing will be discussed in Section 6.2.

Now consider the vegetation–soil interaction terms in eq. (2). The evaporation from bare soil can be expressed as

$$E_{v00} = e_v \theta(y), \tag{14}$$

where e_v is the potential evaporation (i.e. the evaporation rate when $x \to 0$, $z \to 0$ and $y \to \infty$) and $\theta\,(y)$ is a function dependent on the soil wetness and varies from 0 to 1. In this study we take

$$E_{v00} = e_v(1 - \mathrm{e}^{-\varepsilon_{vy}y}), \tag{15}$$

which is the same as Serafini and Sud (1987). While the living leaves cover part of the soil, the wilted leaves are assumed to be distributed uniformly over the soil surface. The latent heat for evaporation at a wet surface is approximately in balance with the net radiation energy, because the Bowen ratio (sensible heat flux to the latent heat) is small over a wet surface. Further, the attenuation of the solar radiation by the living and wilted biomass follows the exponential law (Beer's law). Therefore, the evaporation rate from the soil surface covered only by the wilted biomass is

$$E_{v0} = E_{v00}\mathrm{e}^{-\varepsilon_{vz}z}. \tag{16}$$

For the areas covered by living grass, the solar radiation undergoes attenuation by the living foliage. Thus the evaporation rate from the soil surface shaded by both the living and the wilted biomass is

$$\begin{aligned} E_{v1} &= \left[(1 - \kappa_v) + \kappa_v \mathrm{e}^{-\varepsilon_{vx}x}\right] E_{v0} \\ &= \left[1 - \kappa_v(1 - \mathrm{e}^{-\varepsilon_{vx}x})\right] E_{v0}, \end{aligned} \tag{17}$$

where κ_v is the amplitude of shading effect influenced by living leaves. Hence, the total evaporation can be expressed as the weighted average of E_{v0} and E_{v1}, i.e.

$$\begin{aligned} E_v &= (1 - \sigma_f)E_{v0} + \sigma_f E_{v1} \\ &= e_v(1 - \mathrm{e}^{-\varepsilon_{vy}y})\mathrm{e}^{-\varepsilon_{vz}z} \\ &\quad \times \left\{(1 - \sigma_f) + \sigma_f\left[1 - \kappa_v(1 - \mathrm{e}^{-\varepsilon_{vx}x})\right]\right\}, \end{aligned} \tag{18}$$

where σ_f is the fraction of living grass coverage.

Because transpiration occurs simultaneously with photosynthesis, we assume that E_t can be similarly modelled as G (see eq. 10). Considering the difference of water consumption between the sunlit and non-sunlit leaves, we can use a more general form:

$$E_t = e_t(1 - \mathrm{e}^{-\varepsilon_{ty}y})\sigma_f\left(1 - \kappa_t \mathrm{e}^{-\varepsilon_{tx}x}\right), \tag{19}$$

where e_t is the potential transpiration (i.e. the transpiration rate when $x \to \infty$ and $y \to \infty$) and κ_t is a constant coefficient.

The runoff term considers not only the impact of precipitation and soil wetness, but also of living and wilted leaves as

$$\begin{aligned} R = \lambda P\,(\mathrm{e}^{\varepsilon_{ry}y} - 1)\,\mathrm{e}^{-\varepsilon_{rz}z} \\ \times \left\{(1 - \sigma_f) + \sigma_f\left[1 - \kappa_r(1 - \mathrm{e}^{-\varepsilon_{rx}x})\right]\right\}, \end{aligned} \tag{20}$$

where λ and κ_r are constant parameters.

Finally, the fraction of living grass coverage, σ_f, is described by

$$\sigma_f = 1 - \mathrm{e}^{-\varepsilon_f x}, \tag{21}$$

where ε_f is a coefficient. Note that ε_f could differ from ε_{gx} in eq. (10), depending on the shape and distribution of leaves.

2.3. *Dimensionless state variables and parameters*

For the convenience of mathematical analysis, the state variables and parameters of the model are scaled by proper characteristic values. For example, let x^*, y^* and z^* be the characteristic values of the corresponding state variables, and the dimensionless variables can then be described by $x' = x/x^*$, $y' = y/y^*$ and $z' = z/z^*$, respectively. Theoretically, the dimensionless state variables x' and z' can approach infinity, but y' is bounded. In this study, the values of x', y' and z' are usually within the range of 0 to 2. Similarly the exponential coefficients are replaced by $\varepsilon'_{ku} = \varepsilon_{ku}u^*$ where k denotes the index of a process and u is the corresponding state variable for ε.

Also, the maximum growth rate of the living grass, α, and the potential evaporation, e_v, are used as the dimensional characteristic values of the processes, and denoted as α^* and e^*, respectively. Thus, all other parameters of the model are written in dimensionless form, e.g. $\beta' = \beta/\alpha^*$, $\beta'_z = \beta_z/\alpha^*$, as well as two newly introduced dimensionless water-related parameters,

$$\varphi_{tw} = e_t/e^*, \tag{22}$$

and

$$\mu = P/e^*. \tag{23}$$

This μ is called the "moisture index" in this study. Note that α_z, λ, κ_v, κ_t and κ_r are already dimensionless.

Therefore, the dynamic of the system is described by a set of dimensionless variables and parameters with only five dimensional characteristic values (x^*, y^*, z^*, α^* and e^*), and hence are more convenient for mathematical analyses and numerical simulations. In the following, without causing confusion, we omit the prime on the variables and parameters, and so all terms without an asterisk are dimensionless hereafter.

2.4. Determination of model parameters

In our simplified model both the seasonal and interannual variations are neglected, and all parameters are kept constant. They are determined, either directly or indirectly, by the observational data during the summer time on the Inner Mongolia grassland. However, due to the incompleteness of the data set, some parameters can only be roughly estimated. In this section, we will briefly derive the values of the major parameters. A more detail description can be seen in Zeng et al. (2005).

The living-biomass shading-effect parameter κ_v and potential transpiration ratio φ_{tv} are two of the most important vegetation–soil interaction parameters in the model. By definition (see eq. 18),

$$\kappa_v = \frac{E_v(0,\infty,0) - E_v(\infty,\infty,0)}{E_v(0,\infty,0)}. \tag{24}$$

In general, the evaporation from the land surface

$$e_v \sim \frac{1}{r_{sa}}(p_{vs} - p_{va}), \tag{25}$$

where r_{sa} is surface resistance and p_{va} and p_{vs} are atmospheric and surface vapour pressures, respectively. Assuming r_{sa} does not change much between $E_v(0,\infty,0)$ and $E_v(\infty,\infty,0)$, eqs (24) and (25) yield

$$\kappa_v = \frac{p_{vsat}(T_s^*) - p_{vsat}(T_s^{**})}{p_{vsat}(T_s^*) - RH\, p_{vsat}(T_a)}, \tag{26}$$

where p_{vsat} is the saturation vapour pressure, T_a is the air temperature, T_s^* and T_s^{**} are the soil surface temperatures under the conditions of ($x = z = 0, y \to \infty$) and ($x \to \infty, y \to \infty, z = 0$) respectively, and $RH = p_{va}/p_{vsat}(T_a)$ is the relative humidity.

Transpiration can be treated as a wet surface evaporation under the temperature at the leaf surface. Following a similar derivation, the parameter φ_{tv} is expressed as

$$\varphi_{tv} = \frac{E_t(\infty,\infty)}{E_v(0,\infty,0)} = 1 - \frac{p_{vsat}(T_s^*) - p_{vsat}(T_l^{**})}{p_{vsat}(T_s^*) - RH\, p_{vsat}(T_a)}, \tag{27}$$

where T_l^{**} is the temperature at leaf surface under the condition of $x \to \infty$, $y \to \infty$ and $z = 0$.

While T_a and RH can be directly measured, T_s^*, T_s^{**}, T_l^{**} (all under saturated soil conditions) need to be inferred from data. Over Inner Mongolia, $T_s^* - T_s^{**} \approx$ 5–10 °C, $T_s^* - T_l^{**} \leq 7$ °C and $RH \approx 0.6$ during the summer (personal communication, Xiuming Du, Inner Mongolia Institute of Meteorology). The values of κ_v under different situations of (T_a, T_s^*, T_s^{**}) and φ_{tv} under different (T_a, T_s^*, T_l^{**}) are then calculated by using eqs (24) and (25), where $T_s^* =$ 25–40 °C, $T_s^* - T_a =$ 10–20 °C, $T_s^* - T_s^{**} =$ 5–10 °C, $T_s^* - T_l^{**} =$ 3–7 °C, and $RH = 0.6$. In all cases $\kappa_v =$ 0.3–0.7 and $\varphi_{tv} =$ 0.5–0.7 (for details see Tables 1 and 2, Zeng et al., 2005), and we choose $\kappa_v = 0.4$ and $\varphi_{tv} = 0.6$ in our current study.

According to observational data (Chinese Academy of Sciences, 1985; Jiang, 1988), the fraction of grass coverage in a typical steppe is around 0.5–0.7, and can be as high as 0.9 in some regions. Also, the observations show that after autumn all leaves are wilted and about half of them have accumulated on the ground. We choose the characteristic state variables x^*, y^* and z^* to be the corresponding average values over a natural grassland in Inner Mongolia. Our estimates are $\varepsilon_f = 1$, $\beta = 0.1$, and $\alpha_z =$ 0.5.

Table 1. The characteristic values and parameter values adjusted to the Inner Mongolian grassland. Equation numbers in which the parameters appear are shown in the brackets. (Compared with parameters listed in Table 1 of Zeng et al., 2004, the major modification is ε_{vz} (corresponding to ε_3 in Zeng et al., 2004) which is reduced from 1.0 to 0.8 to reduce the shading effect by wilted biomass. The runoff related parameters, e.g. λ, κ_r, ε_{rx}, are also adjusted in order to prevent an unreasonably large y when $\mu > 0.6$, but such changes have little effect on the bifurcation regime for the range of μ being discussed in this study)

Variable	Characteristic value
x^*	0.1 kg m^{-2}
y^*	240 mm
z^*	0.1 kg m^{-2}
α^*	0.4 kg m^{-2} yr^{-1}
e^*	1000 mm yr^{-1}

Parameter	Value	Eq. nos
β, β_z	0.1	(11), (12)
α_z	0.5	(13)
ε_{gx}, ε_{gy}, ε_{dx}, ε_{dy}	1.0	(10), (11)
ε_{dz}	1.0	(12)
φ_{tv}	0.6	(22)
κ_v	0.4	(18)
κ_t	1.0	(19)
κ_r	0.2	(20)
λ	0.02	(20)
ε_{vx}	0.7	(18)
ε_{vz}	0.8	(18)
ε_{vy}, ε_{tx}, ε_{ty}	1.0	(18), (19)
ε_{rx}	0.4	(20)
ε_{ry}	2.0	(20)
ε_{rz}	0.5	(20)
ε_f	1.0	(21)

Table 2. Eigenvalues of the Jacobian matrix showing the stability of equilibria under moisture index μ. (See Table 1 for the values of the parameters. The critical values $\mu_1 = 0.284$ and $\mu_2 = 0.324$)

μ	Equilibria	Eigenvalues
0.27	0.000, 0.308, 0.000	−0.100, −0.111, −0.754
0.29	0.000, 0.335, 0.000	−0.067, −0.100, −0.738
	0.219, 0.435, 0.298	$0.016, -0.382 \pm 0.11i$
	0.546, 0.537, 0.629	$-0.025, -0.379 \pm 0.29i$
0.31	0.000, 0.362, 0.000	−0.026, −0.100, −0.722
	0.063, 0.395, 0.095	0.016, −0.167, −0.630
	0.758, 0.620, 0.801	$-0.057, -0.394 \pm 0.34i$
0.34	0.000, 0.403, 0.000	0.030, −0.100, −0.699
	0.961, 0.716, 0.947	$-0.087, -0.416 \pm 0.35i$

There are fewer data for estimating other parameters, especially the exponential coefficients. We assigned values to these parameters and justified our assignment by doing sensitivity numerical experiments and fitting the data to the natural situations. Fortunately, many of these parameters are of less importance to the solution.

The values of all the parameters used in this study are listed in Table 1.

3. Stable and unstable equilibrium states of the ecosystem

With different initial values of the state variables (x, y, z), numerical integration of eqs (1) to (3) under given parameters always approaches some equilibrium states. These equilibrium states can be calculated directly by setting $F_1 = F_2 = F_3 = 0$. The behaviour of the system near an equilibrium state is described by the local stability of this equilibrium which can be determined by means of a standard mathematical method (e.g. see Shen, 1993, Section 1.2; Gurney and Nisbet, 1998, Section 3.2). Briefly speaking, eqs (1) to (3) are first linearly expanded around an equilibrium (x_0, y_0, z_0):

$$F_i = \frac{\partial F_i}{\partial x}(x - x_0) + \frac{\partial F_i}{\partial y}(y - y_0) + \frac{\partial F_i}{\partial z}(z - z_0) \quad \text{for i} = 1, 2, 3, \tag{28}$$

where the partial derivatives are taken at the equilibrium, and the eigenvalues and eigenvectors of the corresponding Jacobian matrix at (x_0, y_0, z_0),

$$J = \begin{bmatrix} \partial F_1/\partial x & \partial F_1/\partial y & \partial F_1/\partial z \\ \partial F_2/\partial x & \partial F_2/\partial y & \partial F_2/\partial z \\ \partial F_3/\partial x & \partial F_3/\partial y & \partial F_3/\partial z \end{bmatrix}, \tag{29}$$

are calculated. The matrix might have either three real eigenvalues or one real eigenvalue and a pair of complex conjugate. In our study, the real part of the complex eigenvalue is always negative, so the stability of the equilibrium state is determined by the real eigenvalue(s) only. The equilibrium is stable if each of the real eigenvalues is negative, and the system will return to this equilibrium state from any small perturbations. Otherwise, the equilibrium is unstable and called a saddle, i.e. a small perturbation will normally cause the system to diverge from this state. Each stable equilibrium state corresponds to a possible ecosystem, either grassland or desert, whereas the unstable state is not expected in nature.

The equilibrium states under different values of the prescribed moisture index μ are shown in Fig. 1, and the eigenvalues of some of the equilibrium states are listed in Table 2. There is always a semitrivial equilibrium state of bare soil ($x = z = 0$). This state is stable when μ is less than a critical value μ_2 in Fig. 1, and becomes unstable as $\mu > \mu_2$. The stable equilibrium state of grassland exists when μ is larger than another critical value $\mu_1 < \mu_2$, and the biomass increases continuously with μ. The soil wetness in the grassland is comparatively higher than that in the corresponding desert state under the same μ (Fig. 1b). In the region of $\mu_1 < \mu < \mu_2$ there is also an unstable equilibrium state with a certain amount of living grass. The bifurcation diagram shown in Fig. 1 implies that the ecosystem is a desert when $\mu < \mu_1$, a grassland when $\mu > \mu_2$, and can be either grassland or desert when $\mu_1 < \mu < \mu_2$.

The bifurcation diagram shown in Fig. 1 is well known as hysteresis in physics, that is, when the climatic condition μ decreases across μ_2, the pre-existing grassland can persist with the biomass decreasing smoothly. However, if μ further decreases across the critical point μ_1, the grassland collapses with both the biomass and the soil wetness dropping dramatically, and the grassland ecosystem is replaced by the desert. The desert state will remain even if μ increases later and is above μ_1, and the grassland can be recovered only if μ further increases above μ_2. Because there is no stable equilibrium state for a relatively small amount of biomass, the transition between grassland and desert is abrupt. The value of $|\mu_1 - \mu_2|$ is an important index describing such hysteresis (see Scheffer et al., 2001, for more examples and explanation of hysteresis phenomena in ecosystems).

4. Sensitivity experiments

To check the robustness of the above results, sensitivity tests have been done by changing the values of the model parameters as well as changing the dependency of model processes on the state variables, i.e. the shape of the transformation function $f(u)$ (see eqs 4–6).

4.1. Sensitivity to model parameters

Note that the equilibrium states depend on the dimensionless parameters only, and are not influenced by the dimensional characteristic values (i.e. x^*, y^*, z^*, α^* and e^*). We begin the

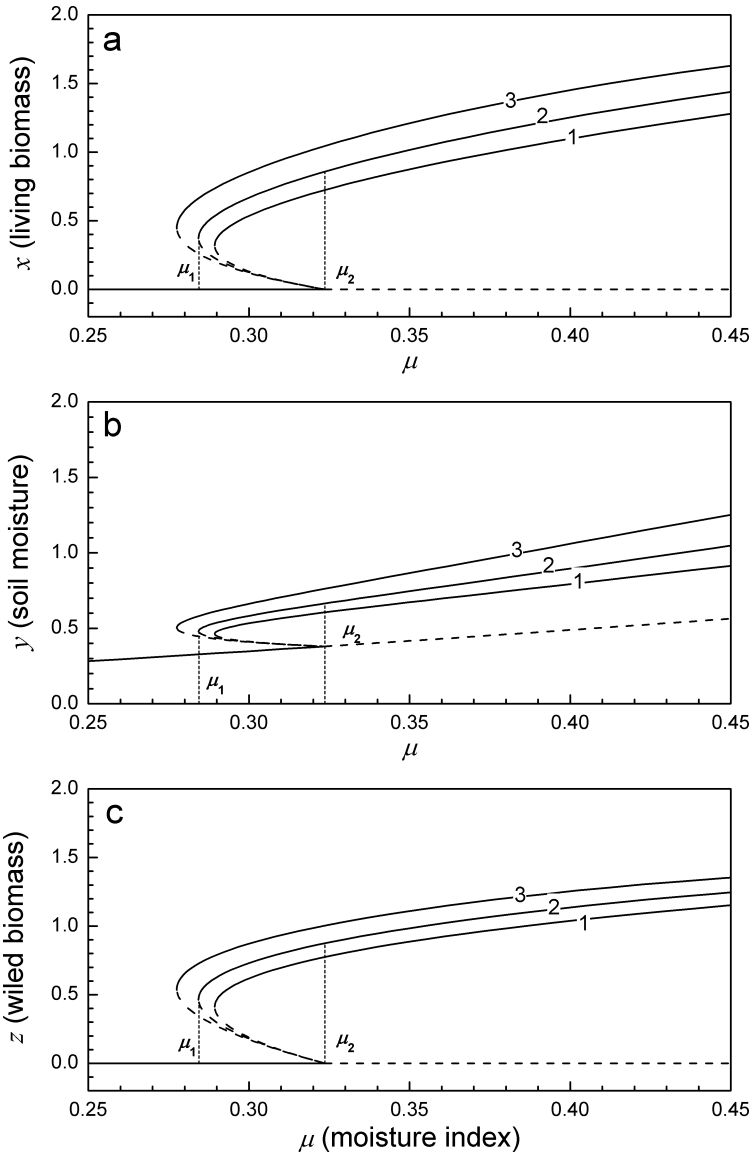

Fig. 1. The equilibrium states of (a) living biomass x, (b) soil wetness y and (c) wilted biomass z as a function of the moisture index μ. The two critical values are indicated as μ_1 and μ_2. Solid and dashed lines refer to the stable and unstable equilibrium states respectively. Curves 1–3 correspond to the cases of $(\kappa_v, \varphi_{tv}) = (0.3, 0.7)$, (0.4, 0.6) and (0.5, 0.5). Values of the other parameters are shown in Table 1.

experiments by changing the value of one particular dimensionless parameter at a time to test its influence on the dynamics of the system. The value of each parameter is changed within a specific range. A value outside this range may lead to unreasonable results (e.g. too small a β or β_z will make the corresponding biomass approach infinity, and too small a ε_{gx} or ε_{gy} will prohibit any growth) or become physically meaningless (e.g. $\varphi_{tv} > 1$, $\kappa_v > 1$, $\kappa_t > 1$). Furthermore, because both y and μ are not very large in this study, the runoff term is small. Hence, the runoff-related parameters (i.e. λ, κ_r, ε_{rx}, ε_{ry} and ε_{rz}) are not tested.

The results can be divided into three categories. For most parameters the bifurcation diagram is preserved. The changes in some of the parameters will result in different critical values of both μ_1 and μ_2. This type of sensitivity is denoted as Class Ia (see Fig. 2a). For some others parameters, only μ_1 changes, and so $|\mu_1 - \mu_2|$ also varies. As the value of the parameter increases (or decreases), μ_1 increases and eventually converges to a maximum value that is smaller than μ_2. This case is denoted as Class Ib (see Fig. 2b). However, the dynamics of the system can change with the wilted-biomass-related parameters, e.g. ε_{vz}, α_z and β_z (we will discuss this phenomenon further in Section 5). For instance, Fig. 2c shows the existence of abrupt transitions for the shading effect coefficient $\varepsilon_{vz} = 0.45$ to 1.0. As ε_{vz} is further reduced below 0.3, however, abrupt transitions no longer occur, and biomass varies smoothly with μ. This type of sensitivity is denoted as Class II. The classification of the dimensionless model parameters is shown in Table 3.

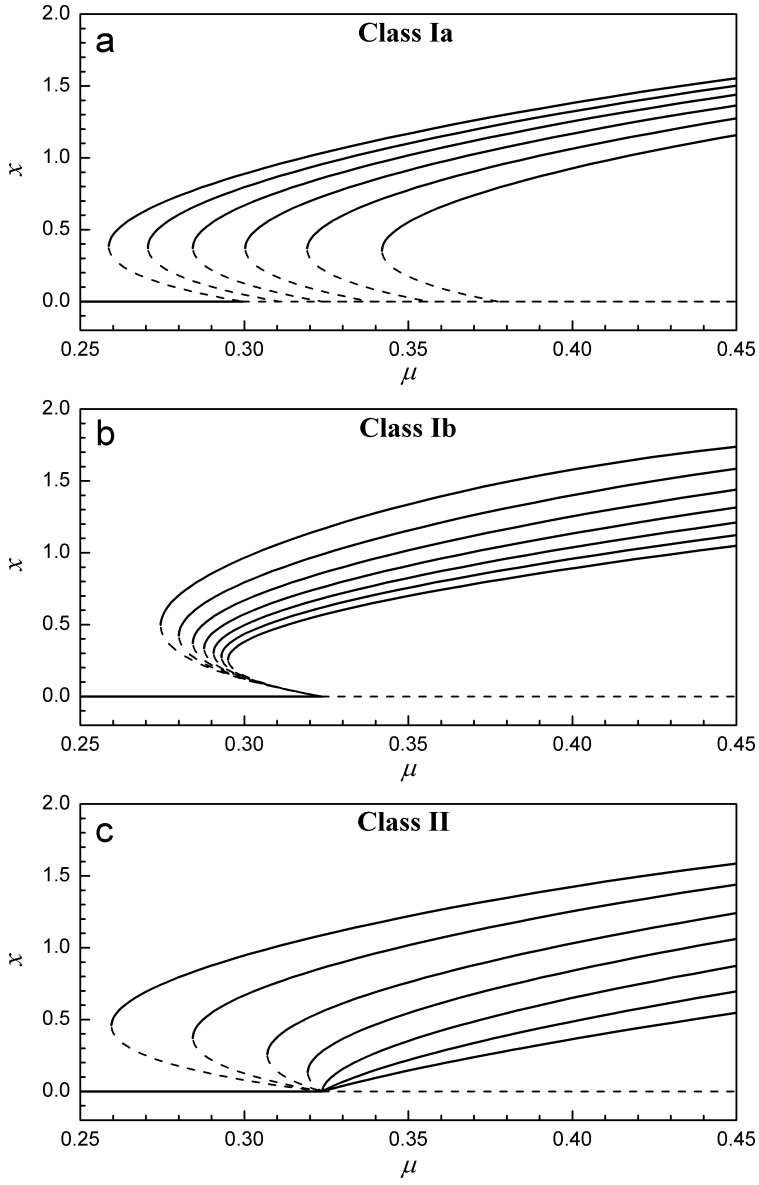

Fig. 2. Sensitivity of the equilibrium states to the parameter (a) ε_{gy} (the exponential coefficient of the growth dependence on the soil wetness), (b) φ_{tv} (the potential transpiration rate) and (c) ε_{vz} (the exponential attenuated coefficient of shading by wilted biomass), show the bifurcation schemes of Classes Ia, Ib and II, respectively. From left to right: (a) $\varepsilon_{gy} = 1.2$, 1.1, 1.0, 0.9, 0.8 and 0.7; (b) $\varphi_{tv} = 0.4$, 0.5, 0.6, 0.7, 0.8, 0.9 and 1.0 and (c) $\varepsilon_{vz} = 1.0$, 0.8, 0.6, 0.45, 0.3, 0.15 and 0. Other parameters are kept the same as those in Table 1.

4.2. Sensitivity to the transformation function f(u)

To investigate the model's sensitivity to the dependency of the process terms on the state variables, the exponential function $f_1(u)$ (eq. 6) used in eqs (10, 11, 13 and 18–20) are replaced by other functions which also satisfy the constraints (4) and (5) and possess the same coefficients of f_{max} and k. For the dimensionless equations, f_{max} can be taken as unity and so can be omitted, and the coefficient k is the corresponding exponential coefficients ε of the process.

Besides the exponential function, two other such functions popularly used in meteorology and ecology are the linear segmental function (e.g. Delworth and Manabe, 1989)

$$f_2(\varepsilon, u) = \begin{cases} \varepsilon u, & \text{if } \varepsilon u < 1 \\ 1, & \text{if } \varepsilon u \geq 1 \end{cases} \tag{30}$$

and the Holling function type II (Gurney and Nisbet, 1998)

$$f_3(\varepsilon, u) = 1 - (1 + \varepsilon u)^{-1} = u/(u + \varepsilon^{-1}). \tag{31}$$

More generally, functions that are subject to the constraints (4) and (5) can be written as

$$f(\varepsilon, u) = 1 - \left(1 + \varepsilon u + \sum_{n=2}^{\infty} a_n u^n\right)^{-1}. \tag{32}$$

Table 3. Classification of the dimensionless model parameters according to the sensitivity of the system dynamics to these parameters. For Classes Ia and Ib, the bifurcation diagram is preserved, but the change of the parameter results in different (or the same) μ_2 for Class Ia (or Class Ib); for Class II, the bifurcation diagram is different (see Fig. 2 for details). The range of values within which the parameter is tested is shown

Sensitivity type	Parameter	Values tested
Class Ia	β	0.05–0.3
	$\varepsilon_{gx}, \varepsilon_{gy}, \varepsilon_{dx}, \varepsilon_{dy}$	0.5–1.5
	ε_{vy}	0.5–1.5
Class Ib	φ_{tv}	0.2–1.0
	$\kappa_v, \kappa_t, \kappa_r$	0–1.0
	ε_f	0.5–1.5
	$\varepsilon_{vx}, \varepsilon_{tx}$	0–1.5
	ε_{ty}	0.5–1.5
Class II	α_z	0–0.8
	β_z	0.05–0.4
	ε_{vz}	0–1.5

For example, the exponential function $f_1(u)$ can be expressed as

$$f_1(\varepsilon, u) = 1 - 1/e^{\varepsilon u} = 1 - \left(1 + \varepsilon u + \sum_{n=2}^{\infty} (\varepsilon^n u^n / n!)\right)^{-1}. \quad (33)$$

In the following study, three additional functions are introduced, for two of which the power series are truncated at orders 2 and 3 respectively, i.e.

$$f_4(\varepsilon, u) = 1 - \left[1 + \varepsilon\left(u + a_{22}u^2\right)\right]^{-1} \quad (34)$$

and

$$f_5(\varepsilon, u) = 1 - \left[1 + \varepsilon\left(u - a_{32}u^2 + a_{33}u^3\right)\right]^{-1}, \quad (35)$$

where a_{22}, a_{32} and a_{33} are positive coefficients, and the third one is modified from the sigmoid function which is commonly used in the nonlinear dynamics study

$$f_6(\varepsilon, u) = (1 - e^{-2\varepsilon u})/(1 + e^{-2\varepsilon u}) = 1 - (1 + \varepsilon u + \frac{1}{2}\sum_{n=2}^{\infty} \frac{(2\varepsilon u)^n}{n!})^{-1}. \quad (36)$$

For the convenience of description, functions $f_1(u)$ to $f_6(u)$ are denoted as exponential, segmental, Holling, power-2, power-3 and sigmoid functions, respectively.

Figure 3 shows the shapes of the different $f(\varepsilon, u)$ as functions of u. Among all these functions, the segmental function and the Holling function are the two most extreme in approaching the saturated limit of $f(u) = 1$. The segmental function is the fastest one to reach the asymptotes line; that is, $f_2(u)$ saturates quickly as u increases. The Holling function, on the other hand, is the slowest one to approach the line, and $f_3(u)$ increases nearly linearly with u for a wide range of u. Besides, $f_2(u) > f_6(u) > f_1(u) > f_3(u)$ for all $0 < u < \infty$, hence the exponential function and the sigmoid function can be regarded as the transitions from the Holling function to the segmental function. For the given coefficients a_{22}, a_{32} and a_{33}, we have $f_4(u) > f_2(u)$ and $f_5(u) < f_3(u)$ as $u \to 0$, so the power-2 and power-3 functions represent somewhat complicated behaviours for the small values of state variables. Thus, functions f_1 to f_6 cover a wide range of functions with the form of eq. (32).

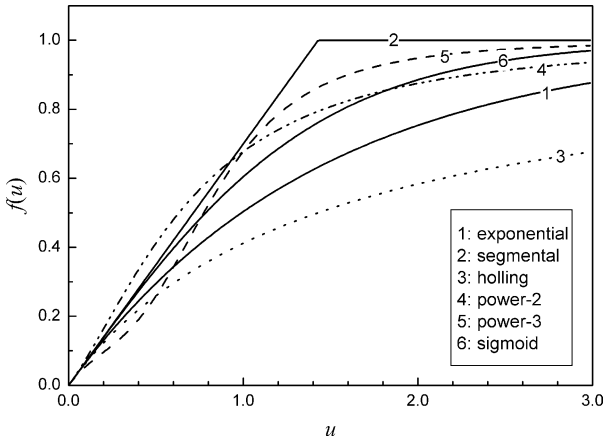

Fig. 3. The sketch of the different functions $f(\varepsilon, u)$ defined in eqs (31)–(36) with $\varepsilon = 0.7$. For curves 4 and 5 the functional coefficients $a_{22} = 2.0$, $a_{32} = 1.0$ and $a_{33} = 4.0$.

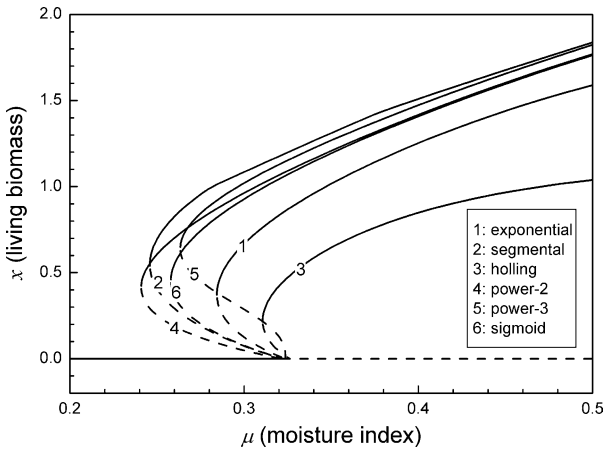

Fig. 4. Sensitivity of the equilibrium states to the different transformation functions as given in Fig. 3.

Figure 4 shows the dynamics of the system responding to functions f_1 to f_6. For all the cases, multiple stable equilibrium states coexist within the semi-arid regions and the bifurcation diagram persists, although the critical values of μ_1 and μ_2 can be different (actually, the variations of μ_2 for these six cases are very small). The value of $|\mu_1 - \mu_2|$ for the case of the segmental function is much larger than that for the Holling function. For the regions near the critical value μ_2, the biomass of the unstable

equilibrium states is smaller for the case of the power-2 function than the segmental function, and is larger for the power-3 function than the Holling function. For a large moisture index $\mu > \mu_2$, the biomass of the stable equilibrium states for the case of the Holling function is relatively smaller due to the comparatively lower value of $f_3(u)$ in the region, while for the other five cases the differences of the biomass are not significant.

5. Self-organization of vegetation and vegetation–soil interaction in semi-arid areas

The mathematical descriptions and theoretical models of ecosystems undergoing abrupt changes between different equilibrium states have been well established (e.g. May, 1977). Here we elucidate the bifurcation diagram from the viewpoint of vegetation–soil interaction.

We first examine the feedbacks in the system. There are positive feedbacks from y to x (eqs 10 and 11), from x and z to y (eq. 18) and from x to z (eq. 12), and negative feedbacks from x to y (eq. 19) and from y to z (eq. 12). The equilibrium state of the system is a balance among these feedbacks.

The variation of living biomass depends on soil wetness only and does not directly depend on the moisture index (or precipitation) and wilted biomass (see eq. 1). To maintain the biomass $x > 0$, a minimum amount of soil wetness (denoted as $y_{\min}$) is required so that $F_1 = G - D - C \geq 0$ (see Fig. 5). For $y < y_{\min}$, F_1 is negative and the living biomass always decreases. For $y > y_{\min}$, the maintenance of a larger amount of biomass x requires a larger amount of soil wetness y, so there is a self-organization of the living biomass towards a balance between growth and wilting.

Now consider the balance of soil water (eq. 2). Let $y_0(\mu)$ be the soil wetness of the equilibrium bare soil state (i.e. $x = z = 0$) under the given moisture index μ. Obviously, $y_0(\mu)$ increases monotonically with μ, and there exists μ_c such that $y_0(\mu_c) = y_{\min}$ (see Fig. 6a). Later we will show that μ_c is actually the critical value μ_2 described in Section 3. For a given μ, the water balance (F_2) is determined by the transpiration by the living biomass and the reduced evaporation due to the shading by both the living and the wilted biomass (the runoff term is negligible when both y and μ are small), and $F_2(x, y, z) = 0$ describes a curved surface in the 3-D phase space of the state variables. For the convenience of illustration, we reduce it to the 2-D profile of $F_2(x, y) = 0$ with the wilted biomass z determined by $F_3(x, y, z) = 0$ (see Fig. 6b).

The intersection points of $F_1 = 0$ and $F_2 = 0$ show the equilibrium states of the system (Fig. 6c). In the region of $\mu > \mu_c$ (e.g. curve 4), the bare soil state holds a sufficient amount of soil water to support the vegetation. So this bare soil equilibrium state is unstable. With a small deviation to this state, i.e. a state with small positive x and z, and $y \sim y_0(\mu) > y_{\min}$, the biomass always grows up and reaches a new equilibrium state with a certain amount of vegetation. On the contrary, in the region of $\mu < \mu_c$ (curves 2 and 3), a small perturbation cannot drive the soil wetness to reach the minimum requirement $y_{\min}$ for the vegetation to be maintained, so that the bare soil state is stable. Hence we have $\mu_c = \mu_2$. Only with a sufficient amount of biomass, especially wilted, will the benefit from the shading through reducing the evaporation be significant and exceed the term of transpiration, so that the soil wetness can be maintained at a level of $y \geq y_{\min} > y_0(\mu)$ for supporting a certain amount of vegetation. With a very low moisture index $\mu < \mu_1$ (curve 1) and thus a relatively small $y_0(\mu)$, the benefit of the shading effect over transpiration is not large enough to maintain the soil wetness above $y_{\min}$, and hence no grassland state is expected. Then the bare soil state is the only equilibrium state, and the ecosystem is a desert.

The coexistence of multiple stable equilibrium states within the semi-arid region requires that the shading reduces evaporation more strongly than the living vegetation promotes the transpiration. This could be achieved through the wilted (dead) biomass because it can provide the benefits of shading without use of the soil water. The wilted vegetation litter covers the soil surface, and so provides a stronger effect by shading than the standing living vegetation. However, in a system with a small accumulation rate (α_z) or a large decomposition rate (β_z) of the wilted biomass, the wilted biomass remains relatively small. Therefore, for $\mu < \mu_2$ the benefit from shading cannot balance the transpiration, so bare soil is the only equilibrium state (Fig. 6d, curves 1 and 2). As $\mu > \mu_2$, $F_1 > 0$ and biomass increases smoothly. In other words, multiple stable equilibrium states cannot coexist for curves 1 and 2 in Fig. 6d (or for the right curves in Fig. 2c).

Note that μ_2 (i.e. μ_c) is determined by $y_{\min}$ (which relates to the grass species parameters) and the water balance on the bare soil. Thus μ_2 only depends on parameters β, ε_{gx}, ε_{gy}, ε_{dx}, ε_{dy}, ε_{vy}, λ and ε_{ry}, and is independent of the parameter of the

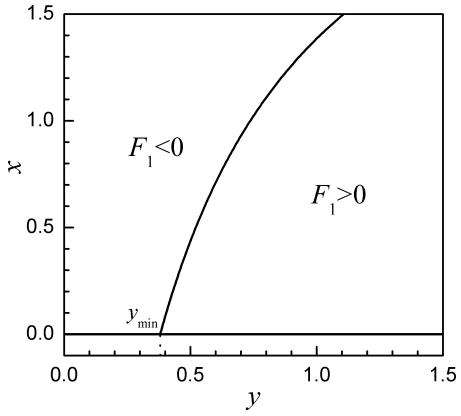

Fig. 5. The dependence of living biomass (x) on soil wetness (y) determined by $F_1 = 0$. Note that $x = 0$ (the bare soil state) is also a solution. A minimum amount of soil wetness (denote as $y_{\min}$) is required for the existence of a solution of $x > 0$.

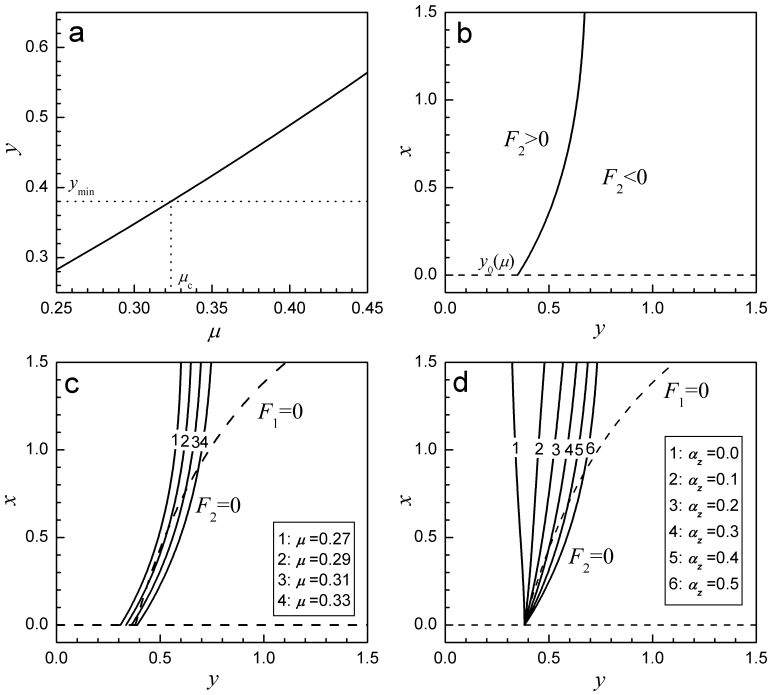

Fig. 6. (a) The dependence of soil wetness (y) on the moisture index (μ) as $x = z = 0$. The critical value μ_c corresponds to the case of $y = y_{min}$. (b) The profile of water balance (F_2) as a function of the living biomass and the soil wetness (y) (the wilted biomass z is determined by setting $F_3(x, y, z) = 0$). Moisture index $\mu = 0.3$. (c) The intersection points of the curve $F_1 = 0$ (dashed line) and $F_2 = 0$ (solid lines) under different prescribed moisture indexes. (d) The intersection points of $F_1 = 0$ and $F_2 = 0$ under different rates of accumulation of wilted biomass $\alpha_z(\mu = \mu_2)$. For comparison, the model parameters in (a)–(c) are kept the same as in curve 2 of Fig. 1, and the corresponding critical values $\mu_1 = 0.284$ and $\mu_2 = 0.324$.

vegetation–soil water feedback and the character of the wilted biomass. The critical value μ_1, on the other hand, depends on the specific shape of curve $F_2 = 0$, and so is related to all model parameters. In particular, some of the wilted-biomass-related parameters affect the monotonicity of the curve $F_2 = 0$, so the bifurcation scheme changes with these parameters. These are consistent with the results discussed in Section 4.1.

6. Grassland maintenance in semi-arid areas

6.1. The attractor basins of the equilibrium states

In the region where both the grassland state and the desert state are stable, the transition between the ecosystems is a matter of concern. Here we address two practical questions: how does the equilibrium state respond to disturbances (e.g. decrease of biomass caused by fire, incidental disease or grazing) and what is the requirement for converting a desert into grassland?

In mathematics, the attractor basin of an equilibrium state describes the region in which all the states will finally approach this equilibrium, say, the region in which the system can recover to this equilibrium from disturbances (see, for example, Fig. 3 in Scheffer et al., 2001, as a sketch map of the concept of attractor basin). When there is plenty of precipitation (i.e. $\mu > \mu_2$), any existing vegetation will grow up and expand, and finally form the stable grassland. This implies that the attractor basin of the grassland state is the whole space of $x > 0$, $y > 0$ and $z \geq 0$. However, this is not the case in the region with $\mu_1 < \mu < \mu_2$. The coexistence of the multiple stable equilibrium states implies that the desert state will remain and not be transformed into a grassland by a relatively small disturbance, and an existing grassland might not be recovered if it undergoes a dramatic decrease in the amount of biomass or soil water. This can be easily elucidated in the phase space of the state variables (x, y, z). The 3-D phase space is divided into three parts according to the attractor basins of the equilibriums. There is a curved surface S on which each state approaches the unstable equilibrium, and the space on one side of this surface belongs to the attractor basin of the equilibrium state of grassland, while the space on the other side belongs to the equilibrium state of desert. To transform a desert to a grassland, state variables must be pushed into the attractor basin of the grassland. An issue of practical importance is what amounts of the biomass (both x and z) are required to form a grassland under a given initial soil wetness y_0. They are determined by projecting the surface S in a 3-D space into a line in a 2-D (x, z) space (see Fig. 7). Obviously, an implant of a certain amount of wilted biomass could reduce the required amount of planted grass. This is another role for the wilted biomass in the grassland ecosystem besides its capability of conserving the soil wetness.

6.2. The issue of grazing

Grazing can be considered as a kind of long-term disturbance. Now we investigate how it influences the dynamics of the system, and how to achieve maximum grazing without exhausting the resources of the grassland.

There is no general law for consumption. When the grassland is grazed by a fixed population of wild herbivores it is often assumed that the consumption C depends on x in the form of a

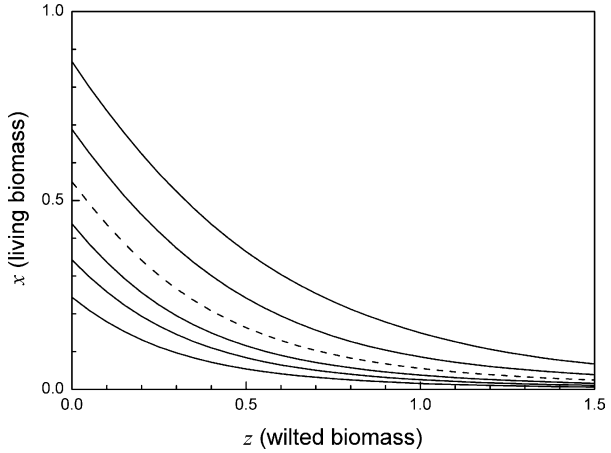

Fig. 7. The minimum requirement of x, y and z to form a grassland. When the initial soil wetness y_0 is given, a minimum amount of living biomass x and wilted biomass z are required so that the ecosystem could finally approach the equilibrium state of a grassland. From top to bottom, for the solid lines, $y_0 = 0.1$, 0.2, 0.5, 0.7 and 1.0, and for the dashed line, $y_0 = 0.335$ (corresponding to the soil water in the bare soil state). Moisture index $\mu = 0.29$. (For comparison, the corresponding unstable equilibrium state is $x = 0.219$, $y = 0.435$ and $z = 0.298$.)

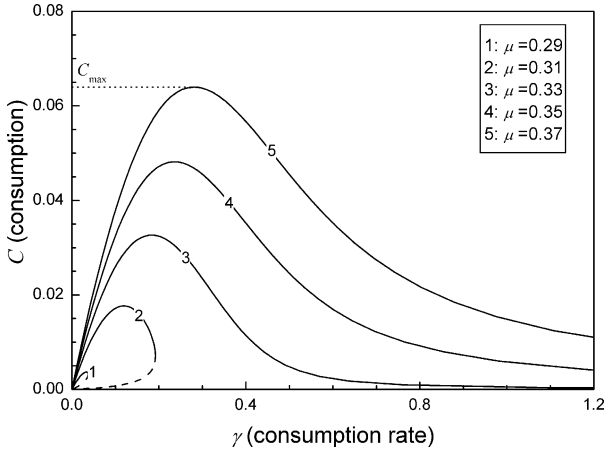

Fig. 8. The grassland products (consumption term C) as a function of the consumption rate γ. Solid and dashed lines refer to the case of stable and unstable equilibrium states respectively (critical value $\mu_2 = 0.324$)). The maximum value for curve 5 is marked by $C_{\max}$.

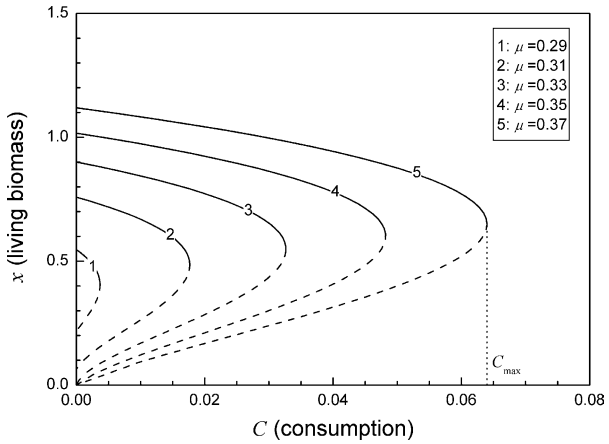

Fig. 9. The equilibrium state of the living biomass as a function of fixed consumption C. For each moisture index μ, there exists a maximum value of consumption, $C_{\max}$, and no grassland is maintained as $C > C_{\max}$ (in this figure $C_{\max}$ for curve 5 is marked).

type II Holling function (Noy-Meir, 1975),

$$C = \gamma x/(x + x_{\mathrm{H}}), \tag{37}$$

where γ is the maximum rate of grazing, and x_{H} is the value of living biomass when $C = \gamma/2$. The sensitivity of the bifurcation scheme of the system to γ belong to Class Ia mentioned in Section 4.1. The case for C_z is similar, but we keep $C_z = 0$ for simplicity.

Under ranching conditions, however, the consumption is controlled by the manager, and it is reasonable to assume that $C(x \to 0) \sim \mathrm{O}(x)$ to favour the recovery of the grassland from a very low amount of living biomass. In such a case, we can take C to be a type III Holling function (May, 1977), or

$$C = \gamma(1 - \mathrm{e}^{-\varepsilon_{\mathrm{cx}} x})^2, \tag{38}$$

and sensitivity of the bifurcation scheme to γ belongs to Class Ib.

Obviously, introducing consumption will disturb the ecosystem and cause the living biomass of the equilibrium state to decrease. With the consumption rate γ increasing, the consumption increases when γ is small, reaches its maximum value at a critical value of γ and then decreases as γ is large (see Fig. 8). In the region of $\mu_1 < \mu < \mu_2$, an overuse of the living grass, i.e. too large a γ, might eventually lead to desertification. In the region of $\mu > \mu_2$, the grassland can be maintained in spite of the value of γ, due to the fact that, when x is small, C is negligible and grass can always grow. However, too large a γ results in small amounts of both biomass and consumption, so it is not an acceptable strategy for grazing.

The definition of C based on x, i.e. eq. (38), may not be a realistic strategy, because it needs frequent inspection of the amount of living biomass. An alternative scheme is to set the consumption C to be a constant and independent of x (unless $x = 0$) on an existing grassland with a sufficient amount of vegetation. Figure 9 shows the equilibrium state of living biomass as a function of C under different values of moisture index. The living biomass decreases as C increases, and no stable grassland can be maintained if C is above a critical value $C_{\max}$, i.e. desertification might occur if the living grass of the grassland is overused. This shows another bifurcation diagram of the system behaviour. Note that the maximum consumptions for different μ are the same as the corresponding values indicated in Fig. 8.

7. Discussion

In this paper we have shown that hysteresis phenomena can occur in the ecosystem with positive feedback between vegetation and soil water. A minimum moisture index (or a minimum amount of annual precipitation) is required for the existence of grassland, and in the semi-arid area multiple equilibrium states (i.e. grassland and desert) coexist in a system with plenty of wilted vegetation. The existing grassland can resist disturbances (such as fire, grazing or human processes) to some extent, but an overuse of the living or wilted grass of the grassland might eventually lead to the stable equilibrium state of a desert, and certain amounts of living and wilted biomass or soil water are required for the recovery of the grassland.

These conclusions are consistent with observations. For example, in Inner Mongolia, vegetation distributions are mainly determined by precipitation (see Fig. 1 of Zeng et al., 2004), and degraded areas (such as sandy land or desert) can appear within the grassland. In the western part, the annual precipitation is less than 300 mm (and moisture index $\mu < 0.3$), and only sparse arid grass or shrubs grows in these regions; while in the eastern part there are typical steppes (or forest-steppe when $\mu \approx 0.6$). The fraction of grass coverage in steppe is around 0.5–0.8, can be as high as 0.9 in eastern regions, and about 0.4 at the edge of the grassland. The biomass is about 600–900 kg hm^{-2} in the region of 300–400 mm of annual precipitation, and 900–2000 kg hm^{-2} when annual precipitation is greater than 400 mm (Jiang, 1988). Sandy lands (with width from 100 m to 100 km) can often be found where the annual precipitation ranges from 300 to 400 mm. The two largest ones are the Hunsandake Desert and the Keerqin Desert, both around 50 000 km^2. The western part of Hunsandake became a desert a long time ago due to wind erosion of sandy soil. There the typical scene consists of wavy sand dunes and shrubs. The degradation of eastern Hunsandake (centred at 116°E and 43°N) was due to over grazing, especially in the last 50 yr. Herds consume the living leaves and also destroy the wilted biomass. Now there appear to be many holes (with diameters of hundreds of metres) of bare sandy soil without vegetation. Some of these holes are connected to each other and extend into the western part of Hunsandake. The height of the remaining grass field of Hunsandake is about 0.2–0.3 m, while in a typical steppe it is 0.5–1.0 m. Keerqin was a high-quality grassland in historical times. However, a large part of it (centred at 121°E and 43°N) was reclaimed for agricultural use in the past 100 yr and now many fields are no longer suitable for cultivation and are degraded into sandy dunes or shrubland.

It is difficult to recover the vegetation in a large area of desert, but people can rebuild the grassland in a small area. A common strategy is to provide for sufficient irrigation. This is equivalent to increasing μ to be larger than μ_2 so that grassland can become established. After that irrigation is stopped, the vegetation can persistently survive there. Another useful experience is to plant in the soil or cover the land surface with dead or wilted leaves. This is often adopted effectively, and irrigation is then needed only for a very short period.

Our study especially emphasizes the impact of wilted biomass in an ecosystem. In a natural grassland with a large amount of living grass there is usually a significant layer of wilted vegetation. But this is not true in a ranch where wilted leaves are often removed by humans or destroyed by herds. Wilted vegetation can provide the benefit of shading without requiring transpiration, so is more effective in conserving soil water. It can also prevent soil from being removed. Despite the importance of wilted biomass in the maintenance of temperate grassland, its dynamical behaviour has been neglected in some land models (e.g. Ek et al., 2003).

As a single-column model, our model describes the hysteresis phenomenon over a large area of well-mixed grassland in arid and semi-arid regions. Horizontal heterogeneity is introduced through the fraction of living grass coverage (i.e. σ_f) and by separately considering processes (e.g. evaporation, transpiration, runoff) over the vegetated and non-vegetated areas in the column. In the transition regions, both biomass and the fraction of grass coverage decrease dramatically. There are also theoretical investigations that explicitly consider the horizontal processes and address the bifurcation phenomena in fine spatial scales (e.g. von Hardenberg et al., 2001; Rietkerk et al., 2002; see Rietkerk et al., 2004 for a review). These studies imply that as the precipitation decreases across a semi-arid region, vegetation coverage goes through a diversity of self-organized patches and varies from homogeneous cover, gaps, labyrinths or stripes and spots to desert. The essential mechanism is that water is concentrated from bare soil into vegetated areas due to spatial interactions. Since our model contains only the soil water averaged over vegetated and non-vegetated areas, the above effect can be largely represented by a larger ε_{gy} (the exponential coefficient of the dependence of growth on the soil wetness) compared with the value in the spatial homogenous solution. Our sensitivity experiment has shown that the bistability regime shifts towards the left as ε_{gy} increases (Fig. 2a), in agreement with the conclusion that vegetation patches can persist on the arid or semi-arid regions where a spatially homogenous solution does not exist (van de Koppel and Rietkerk, 2004). How to combine the results of self-organized patchy vegetation into the mesoscale or large-scale dynamic models is an interesting issue for future research.

We have so far ignored climate variability. We can assume that the annual moisture index μ fluctuates from year to year around its long-term average μ_{ave} with $\mu_1 < \mu_{ave} < \mu_2$. Grass responds more slowly than soil water to the climate change. During drought years (i.e. $\mu < \mu_1$), biomass does not decrease until soil water drops below a certain value, and then suffers a dramatic loss if drought continues. As both living and wilted biomass are small, in the following years with ample rain it takes a long time to restore soil water to a level at which vegetation starts to recover. Our modelling results show that grassland can usually be maintained under such climate forcing, but desertification can be

triggered by a large and long enough perturbation. This kind of transition can also be further studied at shorter timescales (e.g. the seasonal variability of μ). If rain is relatively concentrated in some months and the dry season is severe, soil moisture could be depleted to the wilting point in a month or so, and the grass would be dead in less than 2 months. Thus, it may be possible to have transitions even when the annual average index $\mu > \mu_1$. Of course, under such variability the ecosystem is subjected to more complicated biogeophysical and biogeochemical processes, and no figures based on our simple model are shown here. It is more appropriate to use more comprehensive land surface models (e.g. Bonan et al., 2003) for such studies, whereas our research with a simple model can help to interpret, understand and improve the dynamics and behaviours of more comprehensive models.

8. Acknowledgments

This work was supported by the NSF (ATM0301188), NASA (NNG04GL25G and NAGS-13322), and the China Natural Science Foundation (No. 40233027). SSPS also thanks MITACS (Mathematics of Information Technology and Complex Systems) for a research grant, and the Chinese Academy of Sciences for an Overseas Assessor's research grant and for the Well-Known Overseas Chinese Scholar award. Two anonymous reviewers are appreciated for helpful comments. QCZ also thanks Gang Zhao, Inner Mongolian Agricultural University, for valuable discussions on the problems of grassland and desertification in China.

References

Bonan, G. B., Levis, S., Stitch, S., Vertenstein, M. and Oleson, K. W. 2003. A dynamic global vegetation model for use with climate models: concepts and description of simulated vegetation dynamics. *Global Change Biol.* **9**, 1543–1566.

Brovkin, V., Claussen, M., Petoukhov, V. and Ganopolski, A. 1998. On the stability of the atmosphere-vegetation system in the Sahara/Sahel region. *J. Geophys. Res.* **103**, 31 613–31 624.

Campbell, G. S. and Norman, J. M. 1998. *An Introduction to Environmental Biophysics,* 2nd edn, Springer, New York.

Chinese Academy of Sciences Comprehensive Survey Group of Inner Mongolia and Ningxia Autonomous Regions 1985. *The Inner Mongolia Vegetation.* Science Press, Beijing.

Claussen, M., Kubatzki, C., Brovkin, V., Ganopolski, A., Hoelzmann, P. and co-author 1999. Simulation of an abrupt change in Saharan vegetation in the mid-Holocene. *Geophys. Res. Lett.* **24**, 2037–2040.

Cox, P. M., Betts, R. A., Jones, C. D., Spall, S. A. and Totterdell, I. J. 2000. Acceleration of global warming due to carbon-cycle feedbacks in a coupled climate model. *Nature* **408**, 184–187.

Delworth, T. L. and Manabe, S. 1989. The influence of soil wetness on near-surface atmospheric variability. *J. Climate* **2**, 1447–1462.

Dickinson, R. E., Shaikh, M., Bryant, R. and Graumlich, L. 1998. Interactive canopies for a climate model. *J. Climate* **11**, 2823–2836.

Ek, M. B., Mitchell, K. E., Lin, Y., Rogers, E., Grunmann, P. and co-authors 2003. Implementation of Noah land surface model advances in the National Centers for Environmental Prediction operational mesoscale Eta model. *J. Geophys. Res.* **108**, 8851, doi:10.1029/2002JD003296.

Gurney, W. S. C. and Nisbet, R. M. 1998. *Ecological Dynamics.* Oxford University Press, New York.

Haxeltine, A. and Prentice, I. C. 1996. BIOME3: an equilibrium terrestrial biosphere model based on ecophysiological constraints, resource availability, and competition among plant functional types. *Global Biogeochem. Cycles* **10**, 693–709.

Huntingford, C., Cox, P. M. and Lenton, T. M. 2000. Contrasting responses of a simple terrestrial ecosystem model to global change. *Ecol. Model.* **134**, 41–58.

Jiang, S. 1988. *Methodology for Grassland Ecosystem Investigation.* Agriculture Press, Beijing.

May, R. M. 1977. Thresholds and breakpoints in ecosystems with a multiplicity of stable states. *Nature* **269**, 471–477.

Noy-Meir, I. 1975. Stability of grazing systems: an application of predator–prey graphs. *J. Ecol.* **63**, 459–481.

Oyama, M. D. and Nobre, C. A. 2003. A new climate-vegetation equilibrium state for Tropical South America. *Geophys. Res. Lett.* **30**, 2199, doi:10.1029/2003GL018600.

Rietkerk, M., Boerlijst, M. C., van Langevelde, F., HilleRisLambers, R., van de Koppel, J. and co-authors 2002. Self-organization of vegetation in arid ecosystems. *Am. Nat.* **160**, 524–530.

Rietkerk, M., Dekker, S. C., de Ruiter, P. C. and van de Koppe, J. 2004. Self-organized patchiness and catastrophic shifts in ecosystems. *Science* **305**, 1926–1929.

Scheffer, M., Carpenter, S., Foley, J. A., Folke, C. and Walker, B. 2001. Catastrophic shifts in ecosystems. *Nature* **413**, 591–596.

Serafini, Y. V. and Sud, Y. C. 1987. The time scale of the soil hydrology using a simple water-budget model. *J. Climatol.* **7**, 585–591.

Shen, S. S. P. 1993. *A Course on Nonlinear Waves*. Kluwer Academic Publishers, Boston, MA.

Svirezhev, Y. M. and von Bloh, W. 1997. Climate, vegetation and global carbon cycle: the simplest zero-dimensional model. *Ecol. Model.* **101**, 79–95.

Svirezhev, Y. M. and von Bloh, W. 1998. A zero-dimensional climate-vegetation model containing global carbon and hydrological cycle. *Ecol. Model.* **106**, 119–127.

UNEP (United Nations Environment Programme) 1992. *World Atlas of Desertification*. Edward Arnold, London.

van de Koppel, J. and Rietkerk, M. 2004. Spatial interactions and resilience in arid ecosystems. *Am. Nat.* **163**, 113–121.

von Hardenberg, J., Meron, E., Shachak, M. and Zarmi, Y. 2001. Diversity of vegetation patterns and desertification. *Phys. Rev. Lett.* **87**, 198101.

Wang, G. and Eltahir, E. A. B. 2000a. Biosphere-atmosphere interactions over West Africa, 2. Multiple climate equilibria. *Q. J. R. Meteorol. Soc.* **126**, 1261–1280.

Wang, G. and Eltahir, E. A. B. 2000b. The role of ecosystem dynamics in enhancing the low-frequency variability of the Sahel rainfall. *Water Resour. Res.* **36**, 1013–1021.

Zeng, N. and Neelin, J. D. 2000. The role of vegetation–climate interaction and interannual variability in shaping the African savanna. *J. Climate* **13**, 2665–2670.

Zeng, Q.-C., Lu, P. S. and Zeng, X. D. 1994. Maximum simplified dynamic model of grass field ecosystem with two variables. *Sci. China Ser. B* **37**, 94–103.

Zeng, Q.-C. and Zeng, X. D. 1996a. An analytical dynamic model of grass field ecosystem with two variables. *Ecol. Model.* **85**, 187–196.

Zeng, X. D., Shen, S. S. P., Zeng X. and Dickinson, R. E. 2004. Multiple equilibrium states and the abrupt transitions in a dynamical system of soil water interacting with vegetation. *Geophys. Res. Lett.* **31**, 5501, doi:10.1029/2003GL018910.

Zeng, X. D., Wang, A. H., Zhao, G., Shen, S. S. P., Zeng, X. B. and co-author 2005. Ecological dynamic model of grassland and its practical verification. *Sci. China Ser. C* **48**, 41–48.

Zeng, X. D. and Zeng, Q.-C. 1996b. Two-variable dynamical model of grass field ecosystem with seasonal variation. *Ecol. Model.* **85**, 197–202.